Lithium diffusion in spinel $Li_4Ti_5O_{12}$ and $LiTi_2O_4$ films detected with ^{8}Li β-NMR

Jun Sugiyama,[1,2,*] Izumi Umegaki,[1] Takeshi Uyama,[1] Ryan M. L. McFadden,[3] Susumu Shiraki,[4] Taro Hitosugi,[4,5] Zaher Salman,[6] Hassan Saadaoui,[7] Gerald D. Morris,[7] W. Andrew MacFarlane,[3] and Robert F. Kiefl[7,8]

[1]*Toyota Central Research and Development Laboratories Inc., Nagakute, Aichi 480-1192, Japan*
[2]*Advanced Science Research Center, Japan Atomic Energy Agency, Tokai, Ibaraki 319-1195, Japan*
[3]*Department of Chemistry, University of British Columbia, Vancouver, BC, Canada V6T 1Z1*
[4]*Advanced Institute for Materials Research, Tohoku University, Sendai, Miyagi 980-8577, Japan*
[5]*School of Materials and Chemical Technology, Tokyo Institute of Technology, Tokyo 152-8552, Japan*
[6]*Laboratory for Muon Spin Spectroscopy, Paul Scherrer Institut, CH-5232 Villigen PSI, Switzerland*
[7]*TRIUMF, 4004 Wesbrook Mall, Vancouver, BC, Canada V6T 2A3*
[8]*Department of Physics and Astronomy, University of British Columbia, Vancouver, BC, Canada V6T 1Z1*

(Received 1 February 2017; revised manuscript received 18 May 2017; published 1 September 2017)

Diffusion of Li^+ in (111) oriented thin films of the spinels $Li_4Ti_5O_{12}$ and $LiTi_2O_4$ has been studied with ^{8}Li β-detected NMR in the temperature range between 5 and 310 K. In $Li_4Ti_5O_{12}$, the spin-lattice relaxation rate ($1/T_1$) versus temperature shows a clear maximum around 100 K ($=T_{max}$) which we attribute to magnetic freezing of dilute Ti^{3+} local magnetic moments, consistent with the results of magnetization and muon spin relaxation (μ^+SR) measurements. The decrease in $1/T_1$ with temperature above T_{max} indicates that Li^+ starts to diffuse with a thermal activation energy (E_a) of 0.11(1) eV. In $LiTi_2O_4$, on the contrary, as temperature increases from 200 K, $1/T_1$ increases monotonically up to 310 K. This suggests that Li also starts to diffuse above 200 K with $E_a = 0.16(2)$ eV in $LiTi_2O_4$. Comparison with conventional Li-NMR on $Li_4Ti_5O_{12}$ implies that both β-NMR and μ^+SR sense short-range Li motion, i.e., a jump diffusion of Li^+ to the nearest neighboring sites.

DOI: 10.1103/PhysRevB.96.094402

I. INTRODUCTION

Nuclear magnetic resonance (NMR) is a powerful method to probe matter at the atomic scale. Among its many applications, the study of microscopic diffusion is important. One well-known modern implementation employs pulsed magnetic field gradients to make the NMR (Larmor) frequency ν_0 dependent on the atom's location. Even with a uniform magnetic field, random atomic motion renders the local fields sensed by the nucleus stochastic functions of time. When the rate of such fluctuations exceeds the static linewidth, the resonance exhibits "motional narrowing", a substantial reduction in linewidth from the low temperature static value. When fluctuations are even faster, they begin to have a Fourier component at ν_0, typically in the MHz range. This causes transitions among the nuclear magnetic sublevels, relaxing the ensemble of spins towards the thermal equilibrium Boltzmann distribution. The rate of this "spin-lattice relaxation" $\lambda = 1/T_1$ is determined by the fluctuation spectral density at ν_0, as first discussed by Bloembergen, Purcell, and Pound [1]. Compared to other techniques, such as electrochemical impedance or tracer studies, NMR has important advantages for observing both short-range and long-range motion [2,3]. Since long-range motion is naturally affected by microstructure, such as grain boundaries and interfaces, the intrinsic self-diffusion coefficient can only be estimated from short-range motion in the bulk.

Here we use $1/T_1$ to begin to study the diffusion of Li^+ in thin films of two electrode materials, line phase compounds in the $Li_{1+x}Ti_{2-x}O_4$ series with $x = 0$ and 1/3, $LiTi_2O_4$ and $Li_4Ti_5O_{12}$. However, conventional NMR is generally not sensitive enough to study thin films, so we use implanted hyperpolarized radioactive spin probes instead of stable magnetic nuclei. Signal detection is based on anisotropic radioactive beta decay, where the high energy beta particle ($e^{\pm}$) is emitted in a direction correlated with the spin direction at the instant of decay. This enhances the sensitivity enabling measurements in thin films. Moreover, by varying the probe implantation energy, one can study properties as a function of depth [4,5].

Specifically we use two such probes: the radioisotope $^8Li^+$ and the positive muon (μ^+) and measure spin relaxation and resonances using β detected NMR (β-NMR) and muon spin rotation and relaxation (μ^+SR). While the experiments are similar, the probes are quite different and provide complementary information. Here, μ^+ is not strictly a nucleus, but it behaves as a light isotope of the proton. In particular, in oxides it is typically bound to an oxygen analogous to a hydroxide ion. In the material, in which Li^+ ions are diffusing, $^8Li^+$ is isotopic with the stable mobile Li^+ in the host and $^8Li^+$ β-NMR provides unambiguous information about Li^+ diffusion [6–9]. On the other hand, the muon is a bystander probe of Li^+ diffusion in the host lattice. Its local environment may fluctuate, either because nearby stable Li ions are moving or because the muon itself is moving. As with conventional NMR, diffusional spin relaxation in β-NMR can be masked by the coexistence of electronic magnetism [10,11]. Using the dependence of the muon spin relaxation on the applied magnetic field, one can effectively distinguish magnetism-related relaxation in many cases [12–15]. There are a number of other features that distinguish these probes as discussed further below.

Concerning the implantation damage to samples with ^{8}Li, the daughter ^{8}Be is extremely unstable and immediately decays into two alpha particles [4]. In fact, for Sr_2RuO_4, the ^{8}Li β-NMR relaxation rate is found to be very compatible with

*e0589@mosk.tytlabs.co.jp

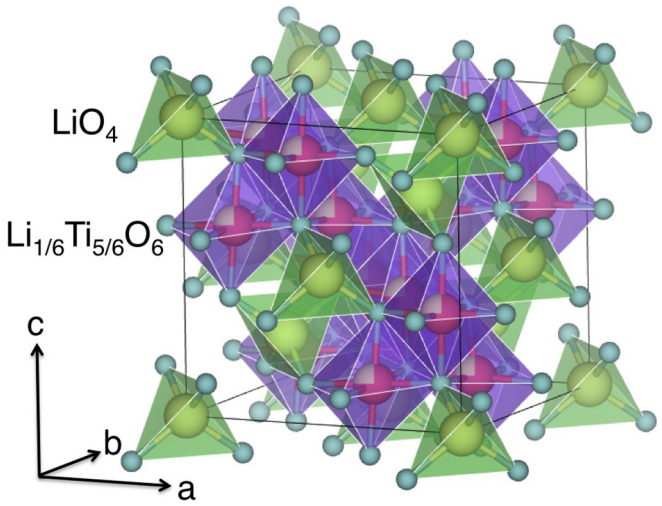

FIG. 1. The crystal structure of spinel $Li_4Ti_5O_{12}$. The tetrahedral A site is occupied by Li^+, while the octahedral B site is occupied by 1/6 Li^+ and 5/6 Ti^{4+}. On the other hand, for $LiTi_2O_4$, the B site is occupied by $Ti^{3.5+}$.

the host lattice NMR, indicating no signs of the implantation damage [17]. In addition, for Fe_2O_3, the transition temperature detected by ^{8}Li β-NMR is the same as the bulk value [16]. Therefore, we will at present ignore such effect on ion diffusion measurements.

We study two materials with the "spinel" crystal structure, members of the series $Li_{1+x}Ti_{2-x}O_4$. At $x = 0$, Ti has an average valence of 3.5, and the material is metallic with a conduction band derived from the Ti $3d$ (t_{2g}) orbitals and becomes superconducting at the relatively high temperature of 13.7 K [18]. With a relatively narrow conduction band, electron correlations are expected to play a significant role in the electronic properties. As x is increased, the metallic state is rapidly destroyed giving way to a dielectric insulator, e.g., $Li_4Ti_5O_{12}$. Aside from the interesting variation in electronic properties, since these materials exhibit good electrochemical properties described below, they are heavily investigated as candidate anode materials for next generation Li ion batteries [19–22].

Key to both the electronic and electrochemical properties is the crystal structure. The spinel ($MgAl_2O_4$) structure of general formula $(A)[B]_2O_4$ has oxide ions on an fcc lattice with A site cations in 1/8 of the tetrahedrally co-ordinated interstitial sites [the Wyckoff 8a sites in the space group $Fd3m$ (No. 227)], and B site cations in 1/2 of the octahedral 16d sites, forming a network of edge sharing octahedra. The resulting cubic unit cell consists of a supercube of eight cubic cells of the fcc oxide sublattice (at $x = 0$ the lattice constant is $a \sim 8.4$ Å) and contains eight formula units. $LiTi_2O_4$ exhibits this structure with slight distortion from the ideal oxide ion positions. When the Li:Ti stoichiometry exceeds 1:2, Li occupies all of the A sites and some of the B sites, e.g., $Li_4Ti_5O_{12}$ is represented by the spinel formula, $(Li^+)[Li^+_{1/6}Ti^{4+}_{5/6}]_2O^{2-}_4$ (see Fig. 1). The reversible Li (de)intercalation reaction is represented by [20,22]

$$(Li^+)_A\left[Li^+_{1/3}Ti^{4+}_{5/3}\right]_B O^{2-}_4 + Li^+ + e^- \rightleftarrows (Li^+_2)_I\left[Li^+_{1/3}Ti^{3+}Ti^{4+}_{2/3}\right]_B O^{2-}_4, \quad (1)$$

where Li^+ ions at the A site are expected to hop to the vacant interstitial I (Wyckoff 16c) sites. The advantage of $Li_4Ti_5O_{12}$ over other materials in battery applications is that the change in lattice constant and working voltage during the reaction in Eq. (1) are very small [19,20], making it a very promising candidate anode material for long cycling lifetimes.

In spite of the demonstrated electrochemical performance, conventional Li-NMR yields extremely small diffusion coefficient of Li^+ (D_{Li}) below 400 K [23–25] consistent with tracer diffusion measurements that find $D_{Li}(\sim 10^{-18}$ cm^2/s) at 300 K [26]. Such a small value means that it should take about one hour to intercalate Li^+ into $Li_4Ti_5O_{12}$ powder with 20 μm diameter, inconsistent with its demonstrated electrochemical behavior [19–22]. In contrast, recent μ^+SR measurements have provided more reasonable D_{Li} ($\sim 3 \times 10^{-11}$ cm^2/s at 300 K) in powder and film samples of $Li_4Ti_5O_{12}$ and $D_{Li} \sim 4 \times 10^{-11}$ cm^2/s in the stoichiometric spinel $LiTi_2O_4$ film [27]. Although D_{Li} for $Li_4Ti_5O_{12}$ has not been calculated from first principles, D_{Li} in the related $LiTi_2O_4$ was predicted to be $\sim 10^{-10}$ cm^2/s [28] consistent with the μ^+SR result. Thus, the diffusivity of Li in $Li_4Ti_5O_{12}$ should be further investigated with the other techniques to resolve this significant discrepancy.

Reversible intercalation of Li^+ is also reported for stoichiometric $LiTi_2O_4$ [19], which is given by [28]

$$(Li^+)_A\left[Ti^{3.5+}_2\right]_B O^{2-}_4 + Li^+ + e^- \rightleftarrows (Li^+_2)_I\left[Ti^{3+}_2\right]_B O^{2-}_4. \quad (2)$$

$LiTi_2O_4$ is thus expected to exhibit a similar diffusive nature to that for $Li_4Ti_5O_{12}$, as recently confirmed using μ^+SR [27]. The lower average valence of the Ti ions (+3.5) compared to $Li_4Ti_5O_{12}$ (+4) results in a lower intercalation voltage by about 0.2 V [19]. The reduced valence also leads its metallic and superconducting properties [18,29] which have been extensively studied [30,31]. However, its electrochemical properties are less investigated than $Li_4Ti_5O_{12}$, as it is not air stable [32].

Diffusion in thin films of both these materials may differ from the bulk due to effects of the interfaces as well as specific structural features, e.g., epitaxial strain. Li diffusion in thin films of these materials is much less well understood, and one of our main motivations for the current study is to elucidate Li ion dynamics in the context of thin films.

Besides the diffusive behavior in $Li_4Ti_5O_{12}$, magnetization and μ^+SR measurements revealed the appearance of localized magnetic moments below 100 K [27,33], although with the nominal Ti valence of 4+, there are no d electrons. In order to explain such moments, we assumed a slight deviation of the Li:Ti ratio from 4:5. That is, the correct formula is rather $Li_{4-y}Ti_{5+y}O_{12}$, resulting in the formation of $3y$ Ti^{3+} ions with $S = 1/2$. Based on the Curie-Weiss behavior of the magnetization at high temperatures ($T > 100$ K), y was estimated to be below 0.08. If this assumption is correct, β-NMR should also detect remarkable relaxation caused by these dilute magnetic moments.

The magnetization measurements on two commercially available $Li_4Ti_5O_{12}$ powders also showed a sudden increase in magnetization below 100 K [33]. This means that the appearance of localized magnetic moments at low temperatures is a common behavior in $Li_4Ti_5O_{12}$. Nevertheless, the

past and recent Li-NMR work has been mainly focused on $1/T_1$ at temperatures above room temperature [23,24,34–36], and, as a result, there is no available Li-NMR data below 200 K. Despite a significant contribution of localized magnetic moments on $1/T_1$ in NMR [10], such magnetic behavior was not recognized in the Li-NMR work. It should be noted that one of the two commercially available samples, for which we measured magnetization [33], was also used for the Li-NMR experiments above 200 K [23,24].

Here, we report the first results of β-NMR measurements on $Li_4Ti_5O_{12}$ and $LiTi_2O_4$ films in the temperature range between 5 and 310 K. We have observed clear evidence of Li diffusion above 150 K in $Li_4Ti_5O_{12}$, whereas not in $LiTi_2O_4$ below 200 K. The obtained results were in a good agreement with the μ^+SR results.

II. EXPERIMENTAL

(111) oriented films of $Li_4Ti_5O_{12}$ and $LiTi_2O_4$ were grown on a spinel $MgAl_2O_4$ (111) substrate using a pulsed laser deposition (PLD) technique at the Advanced Institute for Materials Research of Tohoku University. The spinel substrate ($a = 0.808$ nm) was used due to its relatively good lattice match with both $Li_4Ti_5O_{12}$ ($a = 0.8359$ nm) and $LiTi_2O_4$ ($a = 0.8405$ nm). The thickness of the $Li_4Ti_5O_{12}$ film was 190 nm, while that of the $LiTi_2O_4$ was 220 nm. The preparation and characterization of the two films are described in more detail elsewhere [37] (see Appendix).

The β-NMR spectra were measured using the ^{8}Li beam produced at the Isotope Separator and Accelerator (ISAC) at TRIUMF in Canada. The nuclear spin is polarized using a collinear optical pumping method, producing a spin polarized $^8Li^+$ beam with about 70% polarization. The implanted beam energy (E_{Li}^{im}) was 20 keV, for which the ^{8}Li stops at an average depth of about 120 nm, with only a small fraction residing in the substrate.

In the β decay of ^{8}Li, an electron is emitted preferentially opposite to the direction of the nuclear polarization and is detected by scintillation counters, as in μ^+SR. Therefore, we can measure the change in asymmetry (A) as a function of time for a pulsed beam or as a function of frequency of an applied RF magnetic field with a continuous beam. Here, the time evolution of asymmetry is given by $A(t) = [F(t) - B(t)]/[F(t) + B(t)]$, where $F(t)$ and $B(t)$ are the count rates in the forward and backward counters, respectively. The details of setup and experimental procedure of β-NMR are described elsewhere [4,38–41]. It should be, however, noted that the highest temperature of the present β-NMR spectrometer (310 K) is sometimes too low to detect ionic diffusion in solids [42].

The μ^+SR spectra for the film samples were measured using the low-energy μ^+ (LEM) beam at SμS of PSI in Switzerland. The details of the experiment and the results were described elsewhere [27].

III. RESULTS

A. Spin-lattice relaxation in $Li_4Ti_5O_{12}$

Figure 2 shows the β-NMR time spectrum for the $Li_4Ti_5O_{12}$ film obtained at 5, 100, and 300 K in an applied field of

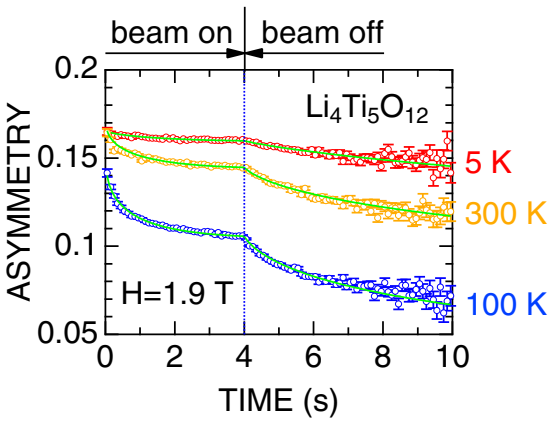

FIG. 2. The asymmetry time spectrum of ^{8}Li in the $Li_4Ti_5O_{12}$ film measured at 5, 100, and 300 K with $H = 1.9$ T. Solid lines represent the best fit of Eq. (3) with $\beta = 1/3$.

1.9 Tesla. The ^{8}Li pulse starts at $t = 0$ and continues for $\delta = 4$ s, resulting in the pronounced kink at $t = \delta$. The β-decay asymmetry is measured both during and after the beam pulse [40]. Due to the longer lifetime of $^8Li^+$ than μ^+, we usually apply a large longitudinal field (1.9 T in this case) perpendicular to the film. As seen in Fig. 2, the relaxation at 100 K is clearly faster than at either 5 or 300 K, indicating a nonmonotonic temperature dependence of the spin-lattice relaxation rate ($1/T_1$). The time spectrum [$A(t) = A_0 P_z(t)$] was best fit by a stretched exponential relaxation function convoluted with the beam pulse, for the fraction of $^8Li^+$ implanted in the sample at t_p [40];

$$A_0\,P_z(t) = A_1 \frac{\int_0^t \exp\left[-\frac{t-t_p}{\tau}\right]\exp\left[-\left(\frac{t-t_p}{T_1}\right)^\beta\right]dt_p}{\int_0^t \exp\left(-\frac{t}{\tau}\right)dt} \qquad t \leqslant \delta,$$

$$A_0\,P_z(t) = A_1 \frac{\int_0^\delta \exp\left[-\frac{\delta-t_p}{\tau}\right]\exp\left[-\left(\frac{\delta-t_p}{T_1}\right)^\beta\right]dt_p}{\int_0^\delta \exp\left(-\frac{t}{\tau}\right)dt} \qquad t > \delta, \tag{3}$$

where A_0 is the initial asymmetry, $P_z(t)$ is the $^8Li^+$ spin polarization function, β is the stretching exponent, and A_1 is the asymmetry for the relaxing signal, and, since we assume a single component decay, $A_0 = A_1$. Although A_1 was not fixed in Eq. (3), it is found to be almost independent of T. We fitted the spectrum at each temperature using Eq. (3) and found that β is almost T independent ($0.2 \leqslant \beta \leqslant 0.4$). However, all the spectra can be adequately described using a common β of 1/3, which we report here.

Figure 3(a) shows the T dependence of $1/T_1$ extracted from the data obtained with $H_0 = 1.9$ and 6.55 T together with the T dependences of the exponential relaxation rate (λ) and muon hop rate (ν) from the previous μ^+SR measurements [Fig. 3(b)] [27] and magnetic susceptibility ($\chi = M/H$) [Fig. 3(c)] [27]. Here, λ for the muon is caused by Ti^{3+} local magnetic moments and ν is rather due to dynamics of the dipolar magnetic fields of the host nuclei at the muon due to Li diffusion. Specifically, the μ^+SR spectrum was fitted by an exponentially relaxing dynamic Gaussian Kubo-Toyabe signal [27], i.e., $\exp(-\lambda t)G^{DGKT}(\Delta,\nu,t)$, since the muon spin is depolarized

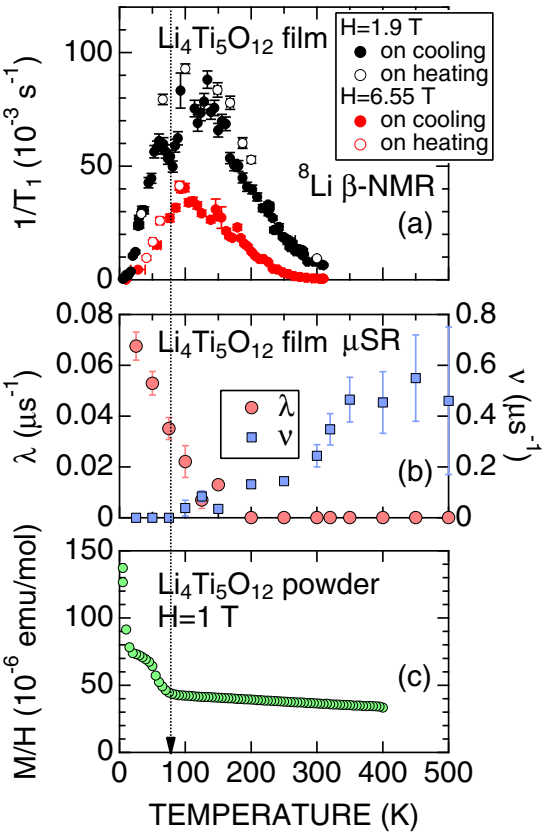

FIG. 3. The temperature dependences of (a) the spin-lattice relaxation rate ($1/T_1$) of ^{8}Li β-NMR with $H = 1.9$ T, (b) the exponential relaxation rate (λ) and the hopping rate (ν) of μ^+SR [27], and (c) magnetic susceptibility (M/H) with $H = 1$ T [27] for $Li_4Ti_5O_{12}$. Both β-NMR and μ^+SR spectra were measured for the film sample, while M was measured for a powder sample. The β-NMR data was obtained by fitting the time spectrum with Eq. (3) and $\beta = 1/3$. The μ^+SR data was obtained by fitting the zero field and weak longitudinal spectra with the exponentially relaxing dynamic Kubo-Toyabe function [27]. The vertical broken line represents the temperature below which the $\boldsymbol{M/H}$ curve deviates from a Curie-Weiss behavior at high temperatures.

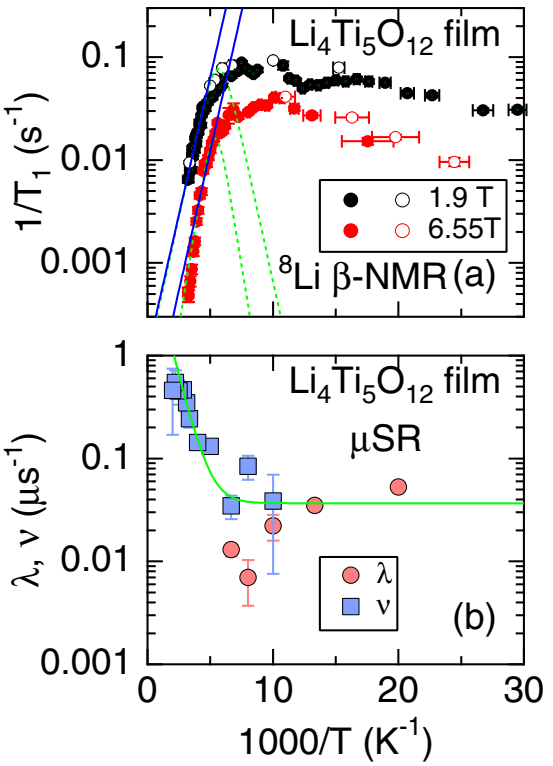

FIG. 4. (a) The spin-lattice relaxation rate ($1/T_1$) and (b) the exponential relaxation rate (λ) and the hopping rate (ν) as a function of inverse temperature for the $Li_4Ti_5O_{12}$ film. In (a), blue solid lines represent the fit results using a thermal activation process, $1/T_1 = A\exp(-E_a/k_BT)$, with $E_a = 0.108(7)$ eV [0.106(4) eV] for the β-NMR data measured with $H = 1.9$ T [6.55 T]. Green broken lines represent a possible BPP relationship, although it is eventually impossible to fit the $1/T_1$ vs T^{-1} curve with BPP due to the absence of a clear maximum. In (b), a green line shows the fit result using a relationship, $\nu = \nu_0 + A\exp(-E_a/k_BT)$, with $E_a = 0.12(2)$ eV for the μSR data.

by both electronic and nuclear magnetic fields. For ^{8}Li $1/T_1$ at both fields exhibits a maximum around 100 K. A peak like this is expected any time a component of the fluctuating local field at the nucleus freezes out. The peak occurs at the temperature where the characteristic fluctuation matches the ^{8}Li NMR frequency $\nu_0 \sim 12{,}42$ MHz at these fields. The $1/T_1$ peaks coincide with the onset of the magnetic relaxation seen by the muon λ rather than the $\chi(T)$ curve, indicating a common origin.

In order to understand the T dependence of $1/T_1$, Fig. 4(a) shows the relationship between $\log[1/T_1]$ and inverse temperature. It is found that the magnitude of the slope at high temperatures (i.e., $1000/T \leqslant 5$), is very large compared with that at low temperatures (i.e., $1000/T \geqslant 10$). This indicates the presence of two different relaxation processes for $1/T_1$. That is, the relaxation due to localized magnetic moments is predominant at low temperatures, while that due to Li diffusion is predominant at high temperatures. We note that, despite the crossover in relaxation mechanism, the shape of the relaxation function in this T range does not change much, resulting in the nearly T-independent β. In addition, since $\chi(T)$ shows the disappearance of localized magnetic moments above 80 K, it is fortuitous that past Li-NMR work above 200 K ignored such a contribution to $1/T_1$. Therefore, we also assume that $1/T_1$ of β-NMR is governed by Li diffusion at high temperatures with no magnetic moments.

Fitting the temperature dependence of $1/T_1$ with the BPP relation [1] is complicated by the presence of the low temperature relaxation due to local moments [see Fig. 4(a)]. Thus, we cannot directly extract a diffusion coefficient of Li^+ (D_{Li}) from the ^{8}Li data, although E_a for Li diffusion is estimated from the fit above ~200 K to a simple thermal activation process, as in the case of a polymer electrolyte [42].

In contrast, since μ^+SR distinguishes the relaxation due to local moments (λ) from that due to Li diffusion (ν), the T dependences of the two parameters were distinguishable as seen in Fig. 4(b). If we assume an Arrhenius-like behavior, $\nu = \nu_0 + A\exp(-E_a/k_BT)$, for the $\nu(T)$ curve in the T range between 50 and 350 K, we estimate $E_a = 0.12(2)$ eV. Here, ν_0 is a T-independent fluctuation rate and k_B is the Boltzmann

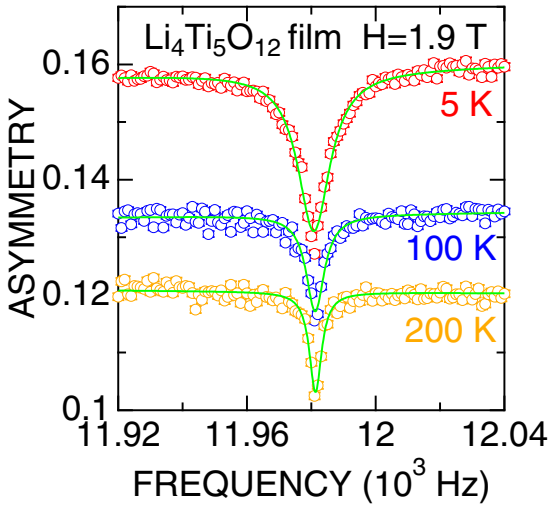

FIG. 5. The nuclear resonance spectra of ^{8}Li for the $Li_4Ti_5O_{12}$ film measured at 5, 100, and 200 K. Solid lines represent the fit using a Lorentz function.

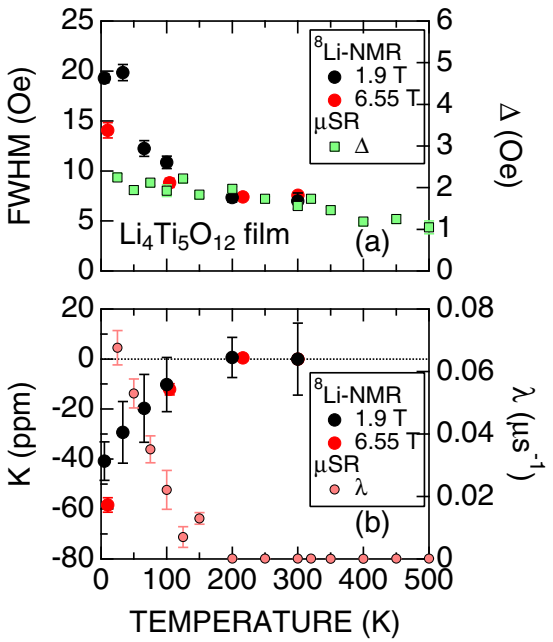

FIG. 6. The temperature dependence of (a) the full width at half maximum (FWHM) of the resonance line and the field distribution width (Δ) and (b) the frequency shift (K) and the exponential relaxation rate (λ) for the $Li_4Ti_5O_{12}$ film. The data of FWHM and F were obtained by fitting the resonance spectrum with a Lorentz function. Δ and λ were obtained from the μ^+SR measurements. For FWHM, 10 Oe corresponds to 6.3 kHz.

constant. The obtained E_a is consistent with the present β-NMR estimates. In addition, this value is comparable with E_a for Li diffusion in $Li_xCoO_2 (x = 0.53 - 0.73)$ estimated with μ^+SR and Li-NMR.

This suggests that μ^+SR senses host Li diffusion in $Li_4Ti_5O_{12}$ and it is not moving itself, as expected in oxides. On the contrary, if muons are diffusing and/or undergoing local reorientation in the vicinity of O^{2-}, E_a should be very small compared with the present β-NMR estimates, as in the case for muon diffusion in metal.

B. Linewidth in $Li_4Ti_5O_{12}$

Figure 5 shows the resonance line for ^{8}Li in the $Li_4Ti_5O_{12}$ film measured at 5, 100, and 200 K with $H = 1.9$ T. Despite the $I = 2$ nuclear spin, there is no indication of a quadrupole splitting even at the lowest T. This implies that the implanted $^8Li^+$ stops at a cubic site(s), where the electric field gradient (EFG) is zero. The resonance line is well fitted by a Lorentzian function in the whole T range, and the linewidth is found to decrease with increasing T.

Figure 6 shows the T dependences of (a) the full width at half maximum (FWHM) and (b) the frequency shift (K) of the resonance. Here, K is defined as $K \equiv [f_r(T) - f_r(300\ \mathrm{K})]/f_r(300\ \mathrm{K})$, where f_r is the resonance frequency at 300 K. In addition, the corresponding μ^+SR parameters, the field distribution width (Δ) and the exponential relaxation rate (λ), are plotted for comparison. Above about 100 K, the ^{8}Li FWHM decreases gradually with T, similar to the muon Δ. Since Δ reflects the dipole field at the muon site mainly caused by Li nuclear spins, the FWHM(T) curve indicates that the nuclear dipolar broadening is predominant at the ^{8}Li site above 100 K. Note that the magnitude of the dipolar linewidth depends on the probe site in the lattice, see Sec. IV B below. We note there is no dramatic motional narrowing up to 300 K, meaning the ^{8}Li hopping rate remains less than 10 kHz throughout the entire observed T range.

At 300 K, the ^{8}Li resonance shift K is small, as expected for Li NMR chemical shifts in a nonmagnetic insulator [43]. In fact, if we compare the measured f_r with that in MgO [44], $K^{\mathrm{vs.MgO}}$ was estimated as about -19 ppm at 300 K. However, it is T dependent, becoming more negative below 200 K, where it seems to track the T dependence of the muon λ. It is possible that this shift simply reflects the demagnetization field due to the perpendicular magnetization of the film at low temperatures [45]. Hyperfine coupling to dilute Ti^{3+} moments would naturally yield a broadening, due to the distribution of distances to the ^{8}Li probe. If, however, the Ti^{3+} are dense enough that there is a uniform component to the susceptibility near the percolation limit of the metallic state, then a hyperfine coupling could result in a resonance shift as was found in the dilute magnetic semiconductor $Ga_{1-x}Mn_xAs$ [46]. Interestingly, K approaches zero ($K^{\mathrm{vs.MgO}} = -19$ ppm), near the temperature where the Li begins to move $T \approx 100$ K. Overall, the resonance results are broadly consistent with the interpretation of $1/T_1$ and the μ^+SR measurements.

C. $LiTi_2O_4$

In order to study the effects of the cation distribution and Ti valence, we also measured ^{8}Li β-NMR in the metallic $LiTi_2O_4$ film. Figure 7 shows the T dependence of $1/T_1$ measured with three different longitudinal fields, 1.0, 1.9, and 6.55 T. Here, we fit the relaxation with Eq. (3) using common $\beta(=1)$, based on a preliminary fit at each T. The difference of β between $LiTi_2O_4$ and $Li_4Ti_5O_{12}$ ($\beta = 1/3$) reflects a more homogeneous distribution of the internal magnetic field at the

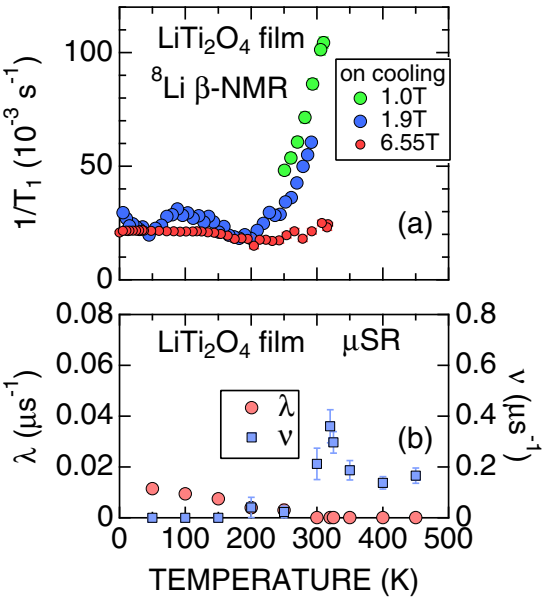

FIG. 7. The temperature dependences of (a) the spin-lattice relaxation rate $(1/T_1)$ of ^{8}Li β-NMR measured with $H = 1.0$, 1.9, and 6.55 T and (b) the exponential relaxation rate (λ) and the hopping rate (ν) of μ^+SR [27] for the $LiTi_2O_4$ film. The data were obtained by fitting the β-NMR time spectrum with Eq. (3) with $\beta = 1$. The range of each axis in (a) and (b) is the same as that for Fig. 3 for comparison.

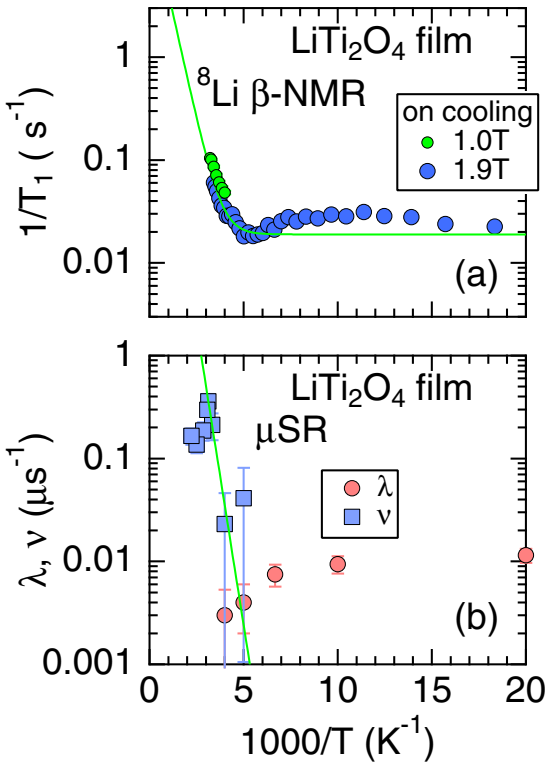

FIG. 8. (a) The spin-lattice relaxation rate $(1/T_1)$ of ^{8}Li β-NMR measured with $H = 1.0$ and 1.9 T and (b) the exponential relaxation rate (λ) and the hopping rate (ν) of μ^+SR [27] as a function of inverse temperature for the $LiTi_2O_4$ film. A solid line in (a) represents the fit result using a thermal activation process for the data with $H = 1.9$ T; namely, $1/T_1 = 1/T_{1,0} + A\exp(-E_a/k_BT)$, where $E_a = 0.16(2)$ eV. In (b), $E_a = 0.17(6)$ eV [27].

^{8}Li site, likely due to the metallic character of $LiTi_2O_4$, which naturally suppresses the formation of localized magnetic moments. Clear at all fields, there is a rapid increase in $1/T_1$ above about 200 K. Below this, however, the relaxation rate is relatively constant. At 1.9 T it shows a small peak at about the same temperature as in the insulating $Li_4Ti_5O_{12}$ followed by a slight low temperature increase. These features appear washed out in the 6.55 T data. It is important to note that the measured rates below 200 K are near the intrinsic lower limit of measurement determined by the radioactive half life of the ^{8}Li probe.

In a metal, one expects that the dominant relaxation will be by spin flip scattering between the nucleus and mobile electrons, giving rise to the characteristic T-linear Korringa law. For example, this is found for implanted ^{8}Li in many simple [4] and even oxide metals [16]. Surprisingly, in $LiTi_2O_4$ we find no T range where $1/T_1 \propto T$. In principle, the magnitude of the Korringa slope depends on the square of the hyperfine coupling to the mobile Ti t_{2g} electrons, and this coupling may simply be very small. For a metal, the ^{8}Li $1/T_1$ is also remarkably slow, e.g., at 300 K it is comparable to the very slow Korringa relaxation we find in semimetallic bismuth [47]. A very small Korringa slope for ^{8}Li is also found in the layered $NbSe_2$, where it is thought to occupy a site in the van der Waals gap, that naturally results in a very small coupling to the highly two-dimensional conduction electrons [48]. We note that in $LiTi_2O_4$, ^{7}Li NMR at 13.00 MHz (0.785 T) finds a comparable relaxation rate at 300 K, and a linear T dependence down to 20 K [49], while away from $x = 0$, deviation from this Korringa slope is evident below about 200 K. In contrast, the increase in $1/T_1$ above 200 K cannot be Korringa relaxation because it is neither T linear nor independent of the applied field.

The strong field dependence above 200 K indicates this relaxation is likely diffusion related. The applied field determines the NMR frequency, and the maximal relaxation rate occurs when the ^{8}Li hopping rate matches ν_0. At all fields this maximum appears to be offscale to higher temperature, beyond the accessible range. Without observing the maximum, it is impossible to measure D_{Li} directly, as in the case of poly-ethylene-oxide [42]. However, the onset of relaxation implies the hopping rates approach the Hz range at 300 K, being consistent with ^{7}Li-NMR [49].

In contrast, our previous μ^+SR measurements on the $LiTi_2O_4$ film [27] provided the T dependences of λ and ν, separately [see Fig. 7(b)], as in $Li_4Ti_5O_{12}$. From the $\nu(T)$ curve and the structural data, we could estimate D_{Li} [27]. In order to confirm the origin of the T dependences of $1/T_1$ and ν, Fig. 8 shows both $1/T_1$ and ν as a function of inverse temperature from which (above 200 K) E_a was estimated to be 0.16(2) eV and 0.17(6) eV [27], respectively. This demonstrates that both β-NMR and μ^+SR detect Li diffusion at temperatures above 200 K.

Figure 9(a) shows the T variation of the resonance spectrum acquired with $H = 1.9$ T and the T dependences of the FWHM and the shift K for ^{8}Li in $LiTi_2O_4$. Since $LiTi_2O_4$ enters the superconducting state below $T_c(H = 0) = 13.7$ K

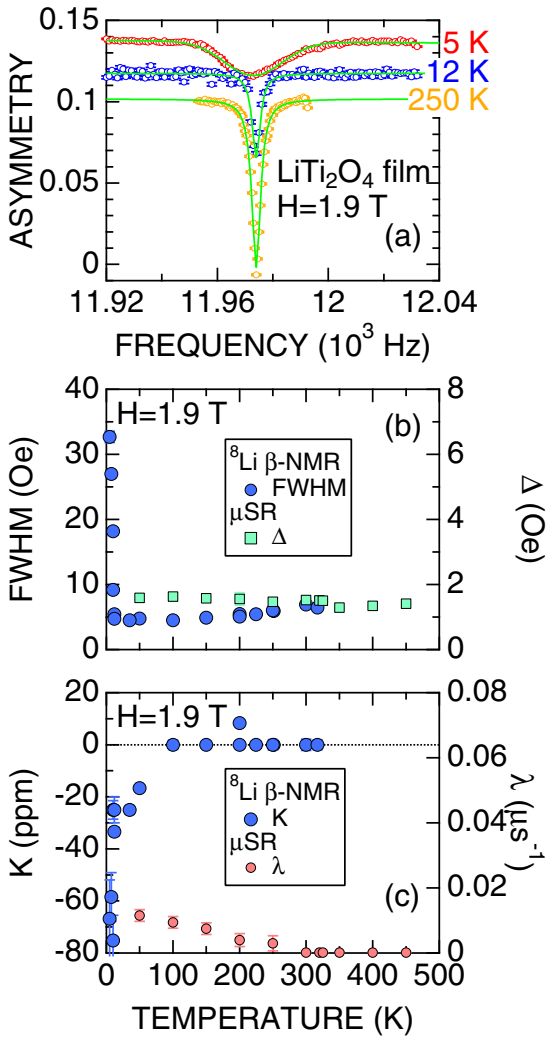

FIG. 9. (a) The nuclear resonance spectra of ^{8}Li for the $LiTi_2O_4$ film measured at 5, 12, and 250 K, and the temperature dependences of (b) FWHM and (c) K. The data in (b) and (c) were obtained by fitting the resonance spectrum with a Voigt function. Such fit results are plotted in (a) as a green solid line. Δ and λ obtained from the μ^+SR measurements [27] are also plotted for comparison.

[18], the resonance line changes dramatically both in shape and width below T_c which is slightly suppressed by the high applied field. The line shape obtained at the lowest T reached (5 K) is asymmetric, as in the case for superconducting $NbSe_2$ [50], consistent with the inhomogeneous magnetic field of the vortex state [51,52]. Since the superconductivity is not of primary interest here, we simply fit the resonance spectrum phenomenologically with the Voigt profile over the whole temperature range measured.

As seen in Fig. 9(b), the linewidth (FWHM), determined from the Voigt function fits, is almost T independent above T_c, despite the increase in $1/T_1$ above 200 K. In particular, motional narrowing is not observed up to 310 K. This is consistent with the nuclear dipolar field seen by the muon [$\Delta(T)$] which only shows a small steplike change around 330 K due to Li diffusion. In fact, the resonance spectrum obtained at $T > T_c$ is well fitted by a Lorentzian, while that obtained at $T \leqslant T_c$ by a broad Gaussian. Since the linewidth above T_c is quite large (compared to γH_1) and comparable to that for $Li_4Ti_5O_{12}$, RF power broadening plays only a minor role in determining the width.

The resonance shift in $LiTi_2O_4$ is very small at $T \geqslant 100$ K, similar to $Li_4Ti_5O_{12}$. This is again remarkable for a metal, which usually exhibits a Knight shift of the NMR due to coupling to the Pauli susceptibility of the conduction electron spins. A very small shift is, however, consistent with ^{7}Li NMR measurements (2.5 ppm [53]) and also with a very small Korringa slope. Below 100 K, the shift becomes negative. This may also be the demagnetization effect proportional to the bulk magnetic susceptibility χ mentioned above. A contribution to χ from local moments on Ti ions may account for both this and the low temperature increase in the muon λ. Below this there is also a rapid decrease in K below T_c [see Fig. 9(c)], due to superconducting diamagnetism, as seen in, e.g., $NbSe_2$ [50].

IV. DISCUSSION

Several effects may be present in a thin film that could alter the ionic diffusivity of Li in comparison to the bulk, such as the presence of interfaces, interfacial electric fields, epitaxial strain, and microstructure. However, our results on both these films are compatible with those in bulk powders [27], indicating such effects are at most small.

It should be noted again that the present ^{8}Li β-NMR result is consistent with the μ^+SR result of the film samples. The μ^+SR result of the $Li_4Ti_5O_{12}$ film is essentially the same as the bulk powder sample [27]. Therefore, the present results indicate that the films exhibit bulk Li dynamics, with no strong effect of the finite size or interfaces, in both $Li_4Ti_5O_{12}$ and $LiTi_2O_4$.

A. Comparison with Li-NMR

From the ^{8}Li probe, in $LiTi_2O_4$, we find metallic spin relaxation is negligible, and there appears an onset of diffusive relaxation above about 200 K that is strongly field dependent as expected. Surprisingly, there is little evidence for motional narrowing in this T range. Below 200 K, the relaxation is very slow but shows some interesting field and T dependence. In particular, there is a local maximum near 100 K that is smaller but similar in temperature to the predominant peak seen in the insulating $Li_4Ti_5O_{12}$. The origin of this peak (that is the dominant feature in the $Li_4Ti_5O_{12}$) is not clear, but it is likely connected with dilute paramagnetic defects [54]. Recent magnetization measurements on $Li_4Ti_5O_{12}$ reveal magnetic freezing near 60 K [33], corresponding to the lowest peak in the $1/T_1(T)$ curve obtained with $H = 6.55$ T. Furthermore, since the μ^+SR result on the $Li_4Ti_5O_{12}$ film sample is essentially the same as the bulk powder sample, the most stable phase prepared by a solid state reaction and/or PLD technique is unlikely $Li_4Ti_5O_{12}$ but in fact is $Li_{4-y}Ti_{5+y}O_{12}$ with $y \leqslant 0.08$. This indicates the difficulty to improve the stoichiometry of the $Li_4Ti_5O_{12}$ sample.

The absence of a similar high temperature onset of increasing relaxation due to diffusion in $Li_4Ti_5O_{12}$ is consistent with previous results in bulk powder samples where ^{7}Li NMR revealed [23,24,36] that $1/T_{1\rho}$ starts to increase above 350 K with $E_a = 0.76(2)$ eV and the FWHM(T) curve shows

a motional narrowing behavior also above 350 K. Here, $1/T_{1\rho}$ represents the spin-lattice relaxation rate in the rotating reference frame. However, as mentioned in Ref. [23], below 350 K, both $1/T_1$ and $1/T_{1\rho}$ are governed by short-range and/or local Li motions with low E_a rather than by long-range Li diffusion. In fact, a linear relationship between $1/T_1$ and inverse temperature was observed in the T range between 200 and 350 K with $E_a \sim 0.1$ eV, similar to the ^{8}Li and μ^+SR results presented here, though the activation barriers are somewhat different. Extending the ^{8}Li$^+$measurements up to higher temperatures should reveal more clearly the diffusive relaxation, and we expect to find the characteristic maximum in $1/T_1$.

It should be noted that the hopping rate of Li^+ ions to the nearest neighboring sites is the elementary step of long-range diffusion and is essential for predicting D_{Li} by first principle calculations [28,55,56]. This is another reason that μ^+SR provides more reasonable D_{Li} than Li-NMR for several materials [14,15,57–61], besides the fact that μ^+SR detects the change in a nuclear magnetic field due to Li diffusion even in the materials containing magnetic ions.

B. The ^{8}Li sites

For a quantitative understanding the diffusive behavior of ^{8}Li, we definitely need to know the crystallographic site of the implanted ^{8}Li in the spinel lattice. This is because, if ^{8}Li sits at the A site in Eqs. (1) and (2), we will measure Li diffusion in the stoichiometric materials, i.e., $Li_4Ti_5O_{12}$ and $LiTi_2O_4$. On the other hand, if ^{8}Li sits at I site, we will see Li diffusion in the charged materials, i.e., $Li_{4+z}Ti_5O_{12}$ and $Li_{1+z}Ti_2O_4$, since Li^+ ions intercalated into the spinel lattice electrochemically generally occupy the interstitial I site.

Ion implantation is not a thermal process, and the implanted $^8Li^+$ usually locates in a high symmetry lattice site either a substitutional or interstitial in the host lattice. Since there is no quadrupole splitting, in both of these materials the implanted ^{8}Li site(s) must have cubic symmetry. One contribution to the low temperature resonance linewidth that is characteristic of the lattice site, is the static nuclear dipolar broadening, due to the spins of the host nuclei. This linewidth can be calculated by van Vleck's method of moments for the ideal lattice. In the absence of broadening by other mechanisms this is expected to give a reasonable estimate of the intrinsic linewidth provided the power broadening is relatively small. The dipolar linewidth (e.g., estimated by the van Vleck method using the powder average expression) is a lower limit on the actual width as any charge disorder in the host lattice would also contribute a quadrupolar broadening. The nuclear dipolar field second moment was calculated for the possible sites, and the results are shown in Table I. It should be noted that this calculation doesn't account for lattice distortion around the implanted $^8Li^+$. This would provide a less reliable estimation for interstitial sites than for substitutional sites.

Since $I = 2$ for ^{8}Li, the FWHM is not directly calculated from Δ and $\gamma_{Li} = 0.63018$ kHz/Oe. However, in order to explain the experimental result, in which FWHM for $Li_4Ti_5O_{12}$ exceeds that for $LiTi_2O_4$ between 100 and 300 K, the implanted ^{8}Li is most likely at the 8a site in both spinels at all temperatures. This site assignment is reasonable, because the Li ions at the $A(8a)$ site are electrochemically active [20–22] and are diffusing at high temperatures. On the other hand, since the $I(16c)$ site is occupied by intercalated Li^+, ^{8}Li β-NMR is unlikely to provide information on the diffusive nature of the intercalated Li^+ in both $Li_4Ti_5O_{12}$ and $LiTi_2O_4$. However, since FWHM depends on the orientation in a single crystal sample [62], more accurate estimation of FWHM would be required for the assignment of the implanted ^{8}Li site.

TABLE I. The field distribution width (Δ) at possible ^{8}Li sites in $Li_4Ti_5O_{12}$ and $LiTi_2O_4$. For $Li_4Ti_5O_{12}$, we used a monoclinic supercell with $a = 10.4850$ Å, $b = 6.0277$ Å, $c = 14.9396$ Å, and $\beta = 89.6036°$ [27]. A and B are substitutional sites, while I is an interstitial site.

Material	Site	(x,y,z)	Δ (Oe)
$Li_4Ti_5O_{12}$	$A(8a)$	(0.002,0.000,0.123)	0.948
	$B(16d)$	(0.000,0.500,0.000)	1.027
	$I(16c)$	(0.340,0.000,0.333)	3.723
$LiTi_2O_4$	$A(8a)$	(0.000,0.000,0.000)	0.795
	$I(16c)$	(0.125,0.125,0.125)	3.969

V. SUMMARY

Using spin-polarized low-energy $^8Li^+$, we have measured β-NMR spectra of (111) oriented thin films of spinel $Li_4Ti_5O_{12}$ and $LiTi_2O_4$. In $Li_4Ti_5O_{12}$, the temperature dependence of the spin-lattice relaxation rate ($1/T_1$) shows a maximum at 100 K ($=T_{max}$), below which localized magnetic moments are seen in magnetization and μ^+SR measurements. The decrease in $1/T_1$ above 200 K is most likely due to Li diffusion. However, the coexistence of localized magnetic moments makes it difficult to clarify the change in T_{max} with applied field. Therefore, a diffusion coefficient was not evaluated but the activation energy (E_a) for Li diffusion was estimated as 0.11(2) eV.

On the contrary, for $LiTi_2O_4$, such $1/T_1$ maximum is not observed until the highest reachable temperature for the present setup (~310 K), although $1/T_1$ starts to increase with temperature above around 200 K. This indicates that Li^+ also diffuses above 200 K in $LiTi_2O_4$ with $E_a = 0.11(1)$ eV.

The different temperature dependence of $1/T_1$ between $Li_4Ti_5O_{12}$ and $LiTi_2O_4$ is thought to be mainly caused by the magnitude of localized magnetic moments, which also affects the exponential relaxation rate of the μ^+SR spectrum. Finally, the present ^{8}Li β-NMR results are very consistent with the previous μ^+SR results, confirming that both techniques detect Li diffusion in these spinels.

ACKNOWLEDGMENTS

We thank the staff of TRIUMF (especially the CMMS) for help with the β-NMR experiments. An image involving crystal structure was made with VESTA [63]. T.H. was supported by MEXT KAKENHI Grants No. JP26106502 and No. JP26108702 and JSPS KAKENHI Grants No. JP26246022

and No. JP26610092. This work was supported by MEXT KAKENHI Grant No. JP23108003 and JSPS KAKENHI Grant No. JP26286084.

APPENDIX

In order to confirm the quality of the two films besides structural, optical, and magnetic characterization [37], Fig. 10 shows the cell voltage (E) as a function of capacity for the $Li_4Ti_5O_{12}$ and $LiTi_2O_4$ film samples versus Li metal, i.e., the charge and discharge curves. The measurements were performed using a Li|$LiPF_6$-ethylene carbonate (EC) -diethyl carbonate (DEC) |$Li_4Ti_5O_{12}$ and Li|$LiPF_6$-ethylene carbonate-diethyl carbonate|$LiTi_2O_4$ cells [64]. The (111) oriented films were grown on an Nb-doped $SrTiO_3$ (111) substrate. The thickness of the $Li_4Ti_5O_{12}$ film was 282 nm, while that of $LiTi_2O_4$ film was 283 nm. The electrolyte was 1 M $LiPF_6$ dissolved in EC-DEC (3/7 v/v) solution. The charge and discharge current was 1.5 μA for $LiTi_2O_4$ and 1.1 μA for $Li_4Ti_5O_{12}$. A lower cutoff voltage was 0.8 V and a higher cutoff voltage was 2.5 V for both cells.

The charge curve for $Li_4Ti_5O_{12}$ ($LiTi_2O_4$) is very flat at 1.59 V (1.35 V) in the capacity range between 20 and 160 mAh/g (10 and 180 mAh/g) and is very consistent with the previous powder data [19,20]. Therefore, the composition of the two film samples must be very homogeneous.

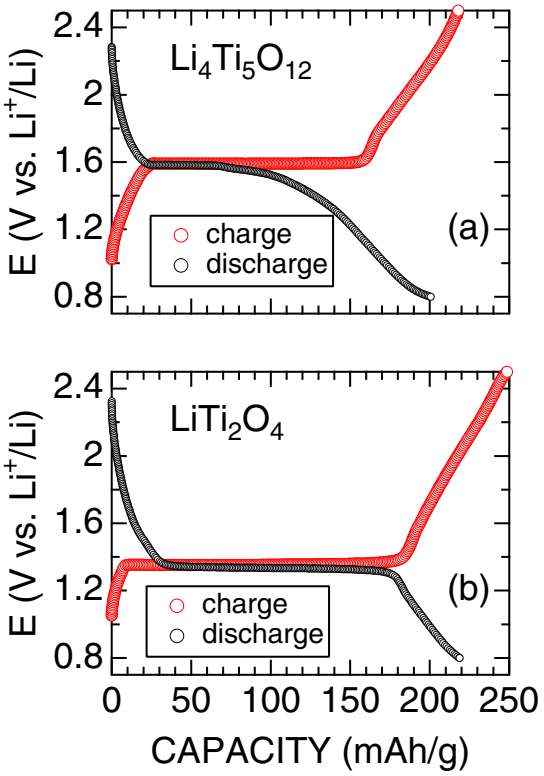

FIG. 10. The charge and discharge curves for (a) the $Li_4Ti_5O_{12}$ and (b) $Li_4Ti_5O_{12}$ films.

[1] N. Bloembergen, E. M. Purcell, and R. V. Pound, Phys. Rev. **73**, 679 (1948).
[2] D. Brinkmann, Prog. Nucl. Magn. Reson. Spectrosc. **24**, 527 (1992).
[3] Edited by P. Heitjans and J. Kärger, *Diffusion in Condensed Matter: Methods, Materials, Models* (Springer Berlin Heidelberg, Berlin, Heidelberg, 2005).
[4] W. MacFarlane, Solid State Nucl. Magn. Reson. **68-69**, 1 (2015).
[5] T. Prokscha, E. Morenzoni, K. Deiters, F. Foroughi, D. George, R. Kobler, A. Suter, and V. Vrankovic, Nucl. Instrum. Methods Phys. Res. Sect. A **595**, 317 (2008).
[6] A. Korblein, P. Heitjans, H. J. Stockmann, F. Fujara, H. Ackermann, W. Buttler, K. Dorr, and H. Grupp, J. Phys. F: Metal Phys. **15**, 561 (1985).
[7] P. Heitjans, W. Faber, and A. Schirmer, J. Non-Cryst. Solids **131-133**, 1053 (1991).
[8] P. Heitjans and S. Indris, J. Phys.: Condens. Matter **15**, R1257 (2003).
[9] B. Ittermann, H. Ackermann, H.-J. Stöckmann, K.-H. Ergezinger, M. Heemeier, F. Kroll, F. Mai, K. Marbach, D. Peters, and G. Sulzer, Phys. Rev. Lett. **77**, 4784 (1996).
[10] C. P. Grey and N. Dupré, Chem. Rev. **104**, 4493 (2004).
[11] K. Nakamura, M. Yamamoto, K. Okamura, Y. Michihiro, I. Nakabayashi, and T. Kanashiro, Solid State Ionics **121**, 301 (1999).
[12] R. S. Hayano, Y. J. Uemura, J. Imazato, N. Nishida, T. Yamazaki, and R. Kubo, Phys. Rev. B **20**, 850 (1979).
[13] T. Matsuzaki, K. Nishiyama, K. Nagamine, T. Yamazaki, M. Senba, J. M. Bailey, and J. H. Brewer, Phys. Lett. A **123**, 91 (1987).
[14] J. Sugiyama, K. Mukai, Y. Ikedo, H. Nozaki, M. Månsson, and I. Watanabe, Phys. Rev. Lett. **103**, 147601 (2009).
[15] M. Månsson and J. Sugiyama, Phys. Scr. **88**, 068509 (2013).
[16] D. L. Cortie, T. Buck, M. H. Dehn, R. F. Kiefl, C. D. P. Levy, R. M. L. McFadden, G. D. Morris, M. R. Pearson, Z. Salman, Y. Maeno *et al.*, Phys. Rev. B **91**, 241113 (2015).
[17] D. L. Cortie, T. Buck, M. H. Dehn, V. L. Karner, R. F. Kiefl, C. D. P. Levy, R. M. L. McFadden, G. D. Morris, I. McKenzie, M. R. Pearson *et al.*, Phys. Rev. Lett. **116**, 106103 (2016).
[18] D. Johnston, H. Prakash, W. Zachariasen, and R. Viswanathan, Mater. Res. Bull. **8**, 777 (1973).
[19] K. Colbow, J. Dahn, and R. Haering, J. Power Sources **26**, 397 (1989).
[20] T. Ohzuku, A. Ueda, and N. Yamamoto, J. Electrochem. Soc. **142**, 1431 (1995).
[21] T.-F. Yi, L.-J. Jiang, J. Shu, C.-B. Yue, R.-S. Zhu, and H.-B. Qiao, J. Phys. Chem. Solids **71**, 1236 (2010).
[22] X. Sun, P. V. Radovanovic, and B. Cui, New J. Chem. **39**, 38 (2015).
[23] M. Wilkening, R. Amade, W. Iwaniak, and P. Heitjans, Phys. Chem. Chem. Phys. **9**, 1239 (2007).
[24] M. Wilkening, W. Iwaniak, J. Heine, V. Epp, A. Kleinert, M. Behrens, G. Nuspl, W. Bensch, and P. Heitjans, Phys. Chem. Chem. Phys. **9**, 6199 (2007).

[25] W. Schmidt, P. Bottke, M. Sternad, P. Gollob, V. Hennige, and M. Wilkening, Chem. Mater. **27**, 1740 (2015).
[26] S. Takai, M. Kamata, S. Fujine, K. Yoneda, K. Kanda, and T. Esaka, Solid State Ionics **123**, 165 (1999).
[27] J. Sugiyama, H. Nozaki, I. Umegaki, K. Mukai, K. Miwa, S. Shiraki, T. Hitosugi, A. Suter, T. Prokscha, Z. Salman *et al.*, Phys. Rev. B **92**, 014417 (2015).
[28] J. Bhattacharya and A. Van der Ven, Phys. Rev. B **81**, 104304 (2010).
[29] D. C. Johnston, J. Low Temp. Phys. **25**, 145 (1976).
[30] K. Jin, G. He, X. Zhang, S. Maruyama, S. Yasui, R. Suchoski, J. Shin, Y. Jiang, H. S. Yu, J. Yuan *et al.*, Nat. Commun. **6**, 7183 (2015).
[31] S. Maruyama, J. Shin, X. Zhang, R. Suchoski, S. Yasui, K. Jin, R. L. Greene, and I. Takeuchi, Appl. Phys. Lett. **107**, 142602 (2015).
[32] F. Xu, Y. C. Liao, M. J. Wang, C. T. Wu, K. F. Chiu, and M. K. Wu, J. Low Temp. Phys. **131**, 569 (2003).
[33] K. Mukai and J. Sugiyama, Phys. Chem. Chem. Phys. **17**, 22652 (2015).
[34] M. Wagemaker, E. R. H. van Eck, A. P. M. Kentgens, and F. M. Mulder, J. Phys. Chem. B **113**, 224 (2009).
[35] H. Hain, M. Scheuermann, R. Heinzmann, L. Wunsche, H. Hahn, and S. Indris, Solid State Nucl. Magn. Reson. **42**, 9 (2012).
[36] W. Schmidt and M. Wilkening, Solid State Ionics **287**, 77 (2016).
[37] A. Kumatani, T. Ohsawa, R. Shimizu, Y. Takagi, S. Shiraki, and T. Hitosugi, Appl. Phys. Lett. **101**, 123103 (2012).
[38] Z. Salman, E. P. Reynard, W. A. MacFarlane, K. H. Chow, J. Chakhalian, S. R. Kreitzman, S. Daviel, C. D. P. Levy, R. Poutissou, and R. F. Kiefl, Phys. Rev. B **70**, 104404 (2004).
[39] G. D. Morris, W. A. MacFarlane, K. H. Chow, Z. Salman, D. J. Arseneau, S. Daviel, A. Hatakeyama, S. R. Kreitzman, C. D. P. Levy, R. Poutissou *et al.*, Phys. Rev. Lett. **93**, 157601 (2004).
[40] Z. Salman, R. F. Kiefl, K. H. Chow, M. D. Hossain, T. A. Keeler, S. R. Kreitzman, C. D. P. Levy, R. I. Miller, T. J. Parolin, M. R. Pearson *et al.*, Phys. Rev. Lett. **96**, 147601 (2006).
[41] G. D. Morris, Hyperfine Interact. **225**, 173 (2014).
[42] I. McKenzie, M. Harada, R. F. Kiefl, C. D. P. Levy, W. A. MacFarlane, G. D. Morris, S.-I. Ogata, M. R. Pearson, and J. Sugiyama, J. Amer. Chem. Soc. **136**, 7833 (2014).
[43] J. Kartha, D. Tunstall, and J. T. Irvine, J. Solid State Chem. **152**, 397 (2000).
[44] W. A. MacFarlane, T. J. Parolin, D. L. Cortie, K. H. Chow, M. D. Hossain, R. F. Kiefl, C. D. P. Levy, R. M. L. McFadden, G. D. Morris, M. R. Pearson *et al.*, J. Phys.: Conf. Series **551**, 012033 (2014).
[45] M. Xu, M. Hossain, H. Saadaoui, T. Parolin, K. Chow, T. Keeler, R. Kiefl, G. Morris, Z. Salman, Q. Song *et al.*, J. Magn. Reson. **191**, 47 (2008).
[46] Q. Song, K. H. Chow, Z. Salman, H. Saadaoui, M. D. Hossain, R. F. Kiefl, G. D. Morris, C. D. P. Levy, M. R. Pearson, T. J. Parolin *et al.*, Phys. Rev. B **84**, 054414 (2011).
[47] W. A. MacFarlane, C. B. L. Tschense, T. Buck, K. H. Chow, D. L. Cortie, A. N. Hariwal, R. F. Kiefl, D. Koumoulis, C. D. P. Levy, I. McKenzie *et al.*, Phys. Rev. B **90**, 214422 (2014).
[48] D. Wang, M. Hossain, Z. Salman, D. Arseneau, K. Chow, S. Daviel, T. Keeler, R. Kiefl, S. Kreitzman, C. Levy *et al.*, Physica B **374-375**, 239 (2006).
[49] M. Itoh, Y. Hasegawa, H. Yasuoka, Y. Ueda, and K. Kosuge, Physica C: Superconductivity **157**, 65 (1989).
[50] Z. Salman, A. I. Mansour, K. H. Chow, M. Beaudoin, I. Fan, J. Jung, T. A. Keeler, R. F. Kiefl, C. D. P. Levy, R. C. Ma *et al.*, Phys. Rev. B **75**, 073405 (2007).
[51] Z. Salman, D. Wang, K. H. Chow, M. D. Hossain, S. R. Kreitzman, T. A. Keeler, C. D. P. Levy, W. A. MacFarlane, R. I. Miller, G. D. Morris *et al.*, Phys. Rev. Lett. **98**, 167001 (2007).
[52] H. Saadaoui, W. A. MacFarlane, Z. Salman, G. D. Morris, Q. Song, K. H. Chow, M. D. Hossain, C. D. P. Levy, A. I. Mansour, T. J. Parolin *et al.*, Phys. Rev. B **80**, 224503 (2009).
[53] M. Dalton, D. P. Tunstall, J. Todd, S. Arumugam, and P. P. Edwards, J. Phys.: Condens. Matter **6**, 8859 (1994).
[54] M. Harrison, P. Edwards, and J. Goodenough, J. Solid State Chem. **54**, 136 (1984).
[55] A. V. der Ven and G. Ceder, Electrochem. Solid-State Lett. **3**, 301 (2000).
[56] B. Ziebarth, M. Klinsmann, T. Eckl, and C. Elsässer, Phys. Rev. B **89**, 174301 (2014).
[57] J. Sugiyama, Y. Ikedo, K. Mukai, H. Nozaki, M. Månsson, O. Ofer, M. Harada, K. Kamazawa, Y. Miyake, J. H. Brewer *et al.*, Phys. Rev. B **82**, 224412 (2010).
[58] J. Sugiyama, H. Nozaki, M. Harada, K. Kamazawa, O. Ofer, M. Månsson, J. H. Brewer, E. J. Ansaldo, K. H. Chow, Y. Ikedo *et al.*, Phys. Rev. B **84**, 054430 (2011).
[59] J. Sugiyama, H. Nozaki, M. Harada, K. Kamazawa, Y. Ikedo, Y. Miyake, O. Ofer, M. Månsson, E. J. Ansaldo, K. H. Chow *et al.*, Phys. Rev. B **85**, 054111 (2012).
[60] J. Sugiyama, K. Mukai, H. Nozaki, M. Harada, M. Månsson, K. Kamazawa, D. Andreica, A. Amato, and A. D. Hillier, Phys. Rev. B **87**, 024409 (2013).
[61] J. Sugiyama, K. Mukai, M. Harada, H. Nozaki, K. Miwa, T. Shiotsuki, Y. Shindo, S. R. Giblin, and J. Lord, Phys. Chem. Chem. Phys. **15**, 10402 (2013).
[62] F. Ohsumi, K. Matsuta, M. Mihara, T. Onishi, T. Miyake, M. Sasaki, K. Sato, C. Ha, A. Morishita, T. Fujio *et al.*, Hyperfine Interact. **120**, 419 (1999).
[63] K. Momma and F. Izumi, J. Appl. Crystallogr. **44**, 1272 (2011).
[64] S. Shiraki, H. Oki, Y. Takagi, T. Suzuki, A. Kumatani, R. Shimizu, M. Haruta, T. Ohsawa, Y. Sato, Y. Ikuhara *et al.*, J. Power Sources **267**, 881 (2014).